Macromolecules

Volume 38, Number 2 January 25, 2005

Communications to the Editor

Kinetics of Surface Phase Separation for PMMA/SAN Thin Films Studied by in Situ Atomic Force Microscopy

Yonggui Liao, Zhaohui Su, Xianggui Ye, Yunqi Li, Jichun You, Tongfei Shi,* and Lijia An*

State Key Laboratory of Polymer Physics and Chemistry, Changchun Institute of Applied Chemistry, Chinese Academy of Sciences, Changchun 130022, People's Republic of China

Received June 24, 2004
Revised Manuscript Received December 7, 2004

Introduction. Phase separation in polymer blends can occur due to the immiscibility between blend components, resulting in a variety of structures, which are important to many applications ranging from biomedical (e.g., gas separating membrane) to microelectronic device fabrication (e.g., lithography).[1,2] It is known that, after a blend is quenched into a metastable or unstable state, phase separation may proceed either by nucleation and growth (NG) or by spinodal decomposition (SD). The time evolution of SD phase separation can be divided into three stages, namely, the early, intermediate, and late stages. In the early stage, the behavior is well described by Cahn's linearized theory.[3,4] In the intermediate and the late stages, time evolution of phase separating domains is traditionally characterized by the power law $q^*(t) \sim t^{-n}$, where $q^*(t)$ and n are the peak wavenumber and the power exponent characterizing the time evolution. After Lifshitz and Slyozov[5] obtained a scaling exponent $n = 1/3$ considering diffusion effects and Siggia[6] proposed tube hydrodynamic instability with $n = 1$ for the bulk system, various theories and simulations[7−20] and many experiments (especially scattering experiments)[21−30] have been focused on the power law describing the phase separation of polymer blends. However, surface phase separation of polymer thin films is not well investigated. It is well-known that the surface composition and structure as well as the final properties of polymer blends at the surface are often different from those in the bulk due to a surface enrichment of the component with a lower surface energy so as to minimize the total surface energy of the system.[31] In addition, for thin films of polymer blends, the surface composition, and structure depend not only on the surface energy of the components but also on the substrate and the film thickness. Consequently, the evolution of the surface morphology of films on different substrates or with different film thickness may be different. Therefore, a detailed understanding of surface phase separation of thin films, especially the kinetics, is helpful for tailoring surface properties of polymer films. Research on morphology of surface-induced phase separation was well reviewed by Geoghegan and Krausch recently.[32] The validity of using data obtained ex situ to describe the real phase separation is still a question. There may be several reasons for this. The quench process results in a shrinkage of the thin film, which can distort the surface structure; more importantly, the humidity at ambient can affect AFM observation significantly, again distorting the images obtained; last, but not least, a wetting temperature may exist for some polymer blends.[33,34] The in situ AFM technique has been employed in many studies.[35−50] However, there is no report of application of this technique in the investigation of polymer surface phase separation kinetics. PMMA/SAN blends have a lower critical solution temperature (LCST) in the bulk, which results in the films being homogeneous when prepared under ambient conditions and phase-separating at high temperatures.[33,34,51,52] Wang and Composto[33] investigated the interface phase separation kinetics for thin films of deuterated poly(methyl methacrylate) (dPMMA)/SAN after etching dPMMA by ex situ AFM. They proposed the bulklike, late-stage spinodal decomposition for the power exponent $n = 1$ in the very early stage and the capillary wave fluctuations for $n = 1/3$ in the middle

* To whom correspondence should be addressed: e-mail tfshi@ciac.jl.cn or ljan@ciac.jl.cn; Tel +86-431-5262137 or +86-431-5262206; Fax +86-431-5685653.

10.1021/ma0487305 CCC: $30.25
Published on Web 12/22/2004

stage.[33] In another paper, they identified four distinct regimes in film thickness as it decreased from semiinfinite to below the radius of gyration.[51] In a previous work, we obtained the phase diagram for the same system,[52] where we learned that the 50/50 PMMA/SAN blend is miscible at temperatures below 155 °C and undergoes spinodal decomposition at above 170 °C. Both results obtained at room temperature reported by Composto and co-workers[31,34,51] and An and co-workers[52] suggest that a thin PMMA layer can wet the surface of the phase-separated blend. In this study, we report our work on the temporal evolution of surface phase separation of PMMA/SAN blend films with ~130 nm film thickness (~$14R_g$) on the silicon substrate by means of in situ atomic force microscopy (AFM), and the kinetics of the surface phase separation will be discussed. Work on the effect of the film thickness and substrate on the surface phase separation kinetics will be reported in future publications.

Experiment. a. Materials. Poly(methyl methacrylate) (PMMA, M_w = 387 kg/mol, PD = 3.72) and poly(styrene-*ran*-acrylonitrile) (SAN, 30% AN by mass, M_w = 149 kg/mol, PD = 2.66), purchased from Across and Aldrich, respectively, were used without any further purification. The glass transition temperatures of PMMA and SAN, obtained from a differential scanning calorimeter (Perkin-Elmer Diamond DSC) at an elevated rate of 10 °C/min, were 128.7 and 112.0 °C, respectively.

b. Sample Preparation. *Substrate*: Silicon wafers were boiled in a bath of 100 mL of 80% H_2SO_4, 35 mL of H_2O_2, and 15 mL of deionized water for 15 min, rinsed in deionized water, and then blown-dry with compressed nitrogen.[53] *Sample 1*: A 1.0×10^{-2} g/mL 1,2-dichloroethane solution of SAN was spun-cast onto the Si wafer to produce a thin film. The film was dried under vacuum at room temperature. 1 μL of a 1.0×10^{-7} g/mL PMMA solution in acetic acid was spun onto the dry SAN thin film, and the fleck was ~3 mm^2 in size. This sample was prepared for the purpose of identifying the characteristics of PMMA domains and SAN domains. *Sample 2*: Thin blend films of PMMA/SAN were prepared by spin-casting the 1.0×10^{-2} g/mL 1,2-dichloroethane solution of the blend (50:50 wt %) onto the silicon wafer pretreated as described above. The thickness of all films measured by a Bruker D8 Discover X-ray reflectometer was 133.5 ± 10.0 nm.

c. AFM Measurements. The AFM measurements were carried out on a scanning probe microscope (SPA-300HV, Seiko Instruments Inc., Japan) equipped with a temperature-control stage. The temperature reading for the hot stage was calibrated with pure gallium, indium, and tin, whose melting points (T_m) are 30, 156, and 232 °C, respectively. The sample was heated to 115 °C at a rate of 5 °C/min, annealed at that temperature for 10 h to remove residual solvent sufficiently, and then elevated to various temperatures for further analyses, namely 155, 165, 175, and 185 °C. For sample 1, the experiment was only carried out at 175 °C. A control experiment performed at 115 °C showed that the annealing sample did not cause phase separation or surface roughening (not shown here). The in situ topography and phase images were obtained simultaneously by virtue of a tapping mode AFM at a constant temperature (115 °C and the experimental temperatures) under ultrahigh vacuum ($<10^{-4}$ Pa). A silicon tip (purchased from Olympus) with a spring constant of 42 N/m was used. AFM was operated at a scan speed of 2 Hz. To ensure the steadiness of the contrast in the height and phase images and to minimize the influence of height variations on the phase images, the set-point ratio under ultrahigh vacuum was set at 0.96 ± 0.01.

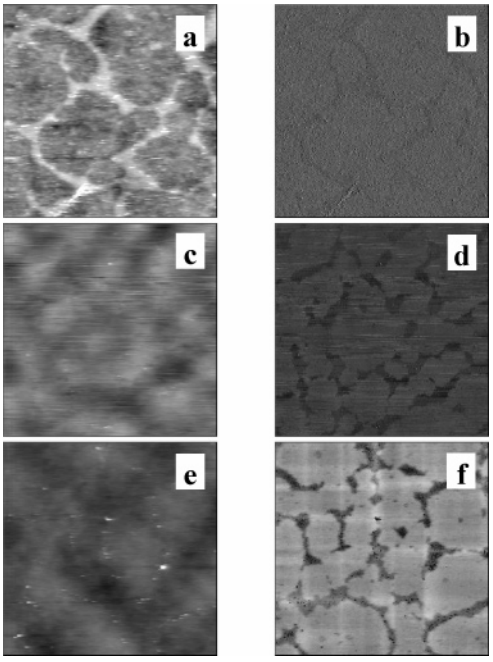

Figure 1. Snapshots of topography (left) and phase (right) images for sample 1: at room temperature (27 °C) under ultrahigh vacuum before treatment (a, b), at 175 °C for 6 min (c, d), and for 244 min (e, f). The *z*-axes for topography and phase images are 8.0 nm and 15.0°, respectively. The dimensions of all images are 5 × 5 μm^2.

The data of root-mean-square surface smoothness (RMS) were directly obtained from topography images of a 5 × 5 μm^2 area using the commercial software bundled with the AFM to ensure that at least one complete protuberance was included, and the data of characteristic wavenumbers, $q^*(t)$, were computed from the phase image of a 2 × 2 μm^2 area as described in the literature,[54] where a further spherical average was performed after the routine 2D fast Fourier transforms (FFT).

Results and Discussion. a. Identification of Domains. Although the evolution of the morphologies can be monitored at different temperatures, the identification of different domains in situ may be a problem. Herein, we try a simple in situ method to identify the different domains on a nanometer scale. Figure 1a shows the topography image of sample 1 under ultrahigh vacuum at room temperature. Because acetic acid is a good solvent for PMMA and a nonsolvent for SAN, when a drop of PMMA solution in acetic acid is cast on a SAN film and dried, as sample 1 was prepared, PMMA must be on top of the SAN film. Therefore, in the topography of sample 1 (Figure 1a) the lighter regions, i.e., the ridges, must be the PMMA phase, and the corresponding regions in the phase image (Figure 1b), the darker regions, can now be identified as PMMA, too. In addition, the amount of PMMA in the 1 μL solution cast on the SAN film was enough to cover only 5% of the 3 mm^2 area (the area covered by the solution) even when it formed a single molecular layer. Therefore, the darker regions, which covered the majority of the surface area, in the topography image of sample 1 cannot be the PMMA phase. This is consistent with the assignment of the domains based on the height data.

To identify the assignment of different regions in the topography and phase images for samples at elevated temperature, we rapidly increased the temperature of sample 1 to the target temperature, which was 175 °C, and monitored the evolution of the surface morphology of sample 1 at this temperature. Figure 1c−f shows the morphologies at the target temperature 175 °C after different annealing times. After 6 min of annealing, in the phase image of the same area of sample 1, two different regions can be clearly observed. Compare with the phase image at room temperature, and it is obvious that the darker domains should be attributed to the PMMA phase, exhibiting a broken netlike morphology, due to the fact that PMMA cannot form a continuous film. In the corresponding topography image (Figure 1c), compared with that at room temperature, it is observed that the PMMA collapses as indicated by the decrease of the height. Furthermore, the topography image for sample 1 at 244 min annealing shows the height decrease, implying PMMA's collapsing further in comparison with that at 6 min (see Figure 1c,e). Moreover, PMMA still maintains the net-broken structure, which can be observed from the phase image (see Figure 1d,f).

b. Morphology and Phase Evolution at Different Annealing Temperatures. Figure 2 shows the snapshots of topography (left) and phase (right) images for a PMMA/SAN (50:50 wt %) thin film after different annealing time at 175 °C under ultrahigh vacuum. The topography images show that the height increases with increasing time during annealing. The phase images change with time in a different way. The phase image is homogeneous when the film is annealed for 21 min. From then on, the surface phase separation starts to develop gradually (see the phase image at 78 min annealing). At 190 min annealing time, this separation is more obvious, and two distinct types of regions, darker and lighter ones, are clearly observed. In addition, an obvious mergence of two neighboring domains of same type was observed at annealing time from 610 to 1255 min, which was highlighted by the circles in Figure 2. From the discussion in the previous section, it has been concluded that in the phase images of PMMA/SAN blends the darker regions are PMMA and lighter ones SAN. Therefore, what we observed is the mergence of PMMA domains takes place.

The evolution of the topography of the blend film annealed at 185 °C, which is not shown here, is similar, except a faster roughening than that for 175 °C. The phase images of sample 2 annealed at different times are shown in Figure 3. They are very similar to that for 175 °C, too. At 6 min annealing, the phase image is homogeneous. From then on, the separation of two regions occurs gradually (see image for 38 min annealing time). At 91 min, the surface phase separation is clearly observed, and two different types of regions, darker and lighter ones, can be readily identified. A mergence of two dark domains (PMMA-rich domains) was also observed when the film was annealed for 225−350 min, which was highlighted by the circles in Figure 3.

c. Kinetics of Surface Phase Separation. To quantitatively analyze the surface phase separation, the root-mean-square surface smoothness (RMS) of the thin binary polymer blend films and the characteristic wavenumber ($q^*(t)$) are introduced.

Figure 4 shows RMS as a function of annealing time for the PMMA/SAN thin films at different annealing temperatures. At 155 °C, the RMS reaches a plateau after an initial slight increase. At higher temperatures, namely, 165, 175, and 185 °C, the RMS increases rapidly and then slows down.

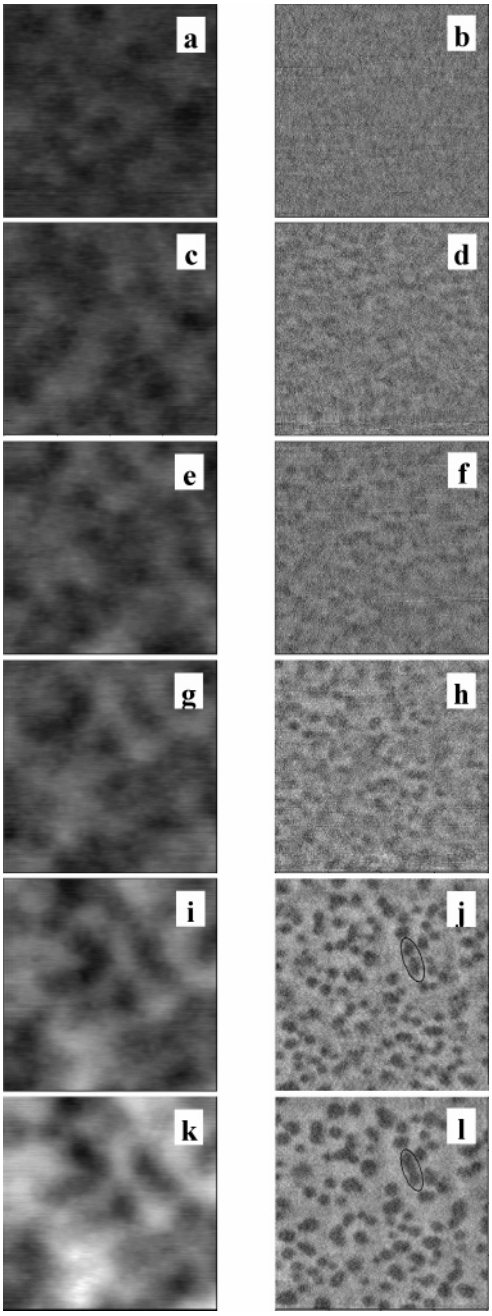

Figure 2. Snapshots of topography (left) and phase (right) images for sample 2 at 175 °C for 21 min (a, b), 78 min (c, d), 190 min (e, f), 290 min (g, h), 610 min (i, j), and 1255 min (k, l). The z-axes for topography and phase images are 10.3 nm and 2.5°, respectively. The dimensions of all images are 2 × 2 μm^2.

Figure 5 shows the time dependence of characteristic wavenumbers ($q^*(t)$) for PMMA/SAN thin films at different annealing temperatures on a log−log scale. For the thin films annealed at 155 and 165 °C, $q^*(t)$ remains constant in the experimental time scale. This indicates that at 155 °C the blends are miscible, and the initial surface roughening might be attributed to thermal fluctuation. At 165 °C an increase of RMS and some fussy domains are observed in the phase images, even though $q^*(t)$ exhibits little variation during entire

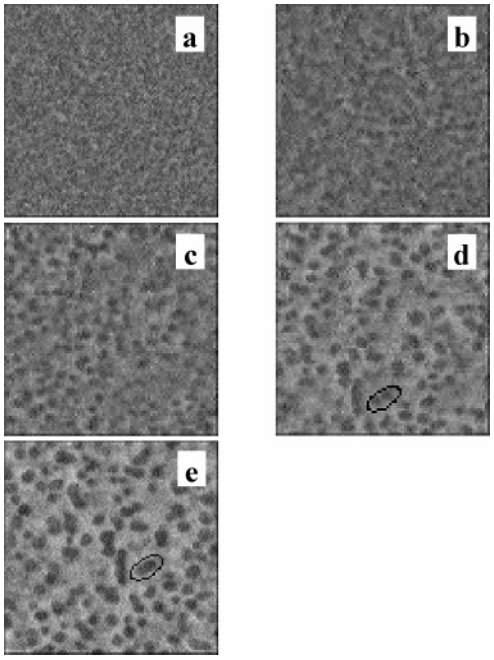

Figure 3. Snapshots of phase images for sample 2 at 185 °C for 6 (a), 38 (b), 91 (c), 225 (d), and 350 min (e). The z-axes are 2.8°. The dimensions of all images are 2×2 μm^2.

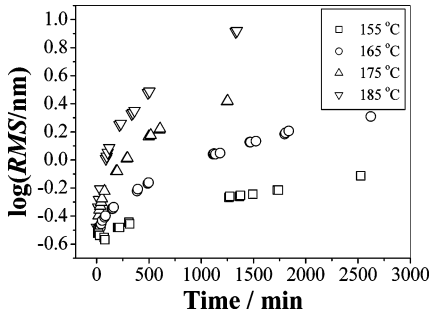

Figure 4. Logarithm of root-mean-square surface smoothness (RMS) as a function of annealing time for sample 2 at different temperatures: 155 (squares), 165 (circles), 175 (up-triangles), and 185 °C (down-triangles). RMS data are obtained from the 5×5 μm^2 topography images.

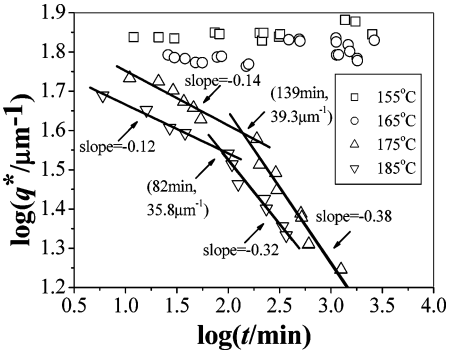

Figure 5. Annealing time dependence of characteristic wavenumbers ($q^*(t)$) for sample 2 at different temperatures: 155 (squares), 165 (circles), 175 (up-triangles), and 185 °C (down-triangles) on a log−log scale. All $q^*(t)$ data are taken from the 2×2 μm^2 phase images.

experimental time scale, suggesting that the 50/50 blends may be near its critical temperature for phase separation. However, at 175 and 185 °C, the $q^*(t)$ as a function of annealing time exhibits two distinct regimes. For the film annealed at 175 °C, $q^*(t)$ follows a power law of $t^{-0.14}$ at the early stage and $t^{-0.38}$ at the later stage, and the two regimes cross at ~139 min and with a crossover $q^*(t)$ of 39.3 μm^{-1}. At 185 °C, the power exponent n is 0.12 in the first regime and 0.32 in the second regime, and the crossover point is at 82 min annealing time and a $q^*(t)$ of 35.8 μm^{-1}. These results indicate that the surface phase separation of PMMA/SAN involves two distinct processes. The power exponent of ~0.13 for $q^*(t) \sim t^{-n}$ in the early stage of surface phase separation is of particular interest because this indicates that the kinetics is much slower than $n = 1$, which has been proposed by Composto on the early stage of an *interface* phase separation process for the same system.[33] On the other hand, there have been other reports on slow phase separation dynamics where n has been found to be ca. 0.13.[28,54] Tanaka[28] investigated phase separation kinetics of polystyrene (PS) in diethyl malonate (DEM) solution by phase contrast microscopy and found that the $q^*(t)$ scaled with $t^{-0.15}$, which is very similar to what we found in this case. He believed that the process was much slower because the pattern evolution was dominated by the slow dynamics of the polymer-rich, viscoelastic phase. In another paper, Ma[54] has obtained a similar power exponent from numerical simulation of the late stage of two-dimensional phase separation of ternary mixtures when wetting strength of one phase (phase C) to another one (phase A or phase B), and the ratios of the interfacial tensions of other two phases (phase A and B) were properly adjusted. In our case, because the surface tension of PMMA is different from that of SAN,[33] for a 50/50 PMMA/SAN blend at an equilibrium state, the surface concentration of one component must be >50%. Therefore, when the film is quickly heated to 175 or 185 °C, which is above the T_g and the critical temperature for phase separation, more polymer chains of this component have to diffuse to the surface to replace the chains of the other component. Maybe this slow process dominates the early stage of the surface phase separation, resulting in a slower kinetics, as indicated by a smaller power exponent, compared to a bulk phase separation. It is also possible that the chain mobility is reduced by the 2D geometry constraint of the surface, which slows down the surface phase separation kinetics. Then, after a period of surface enrichment (incomplete wetting) and phase separation, the RMS is larger, the chains have more freedom to move around, and the enrichment reaches a dynamic equilibrium. Consequently, the phase separation process dominates, and the kinetics can be characterized by the universal power exponent n of ca. $1/3$, i.e., obeying the Lifschitz−Slyozov (LS) law.[5] There are two possible mechanisms for a kinetic process that obeys the LS law, namely Ostwald ripening, i.e., evaporation-condensation, or Brownian diffusion (BD) induced collisions of droplets.[6] Because our system is a polymer blend, it is extremely unlikely that the polymer chains undergo evaporation under our experimental temperature. Therefore, BD is probably the mechanism of the domain growth in the late stage of the surface phase separation. As for the different crossover points at different temperatures, it is probably because the equilibrium of enrichment of faster dynamics at higher temperature, resulting in a shorter crossover time at 185 °C than 175 °C. In this work, we have not reached the late stage of phase separation which is characterized by a zero-order dependence of $q^*(t)$ on t; i.e., the system reaches its equilibrium, which can be investigated by scattering techniques conveniently.[22]

Conclusions. In this report, a novel in situ method to identify different domains with nanometer resolution is established using AFM equipped with a hot stage. The temporal evolution pattern of surface phase separation and its coalescence process for PMMA/SAN blend thin films have been observed using this technique in real space *directly*. The kinetics of the surface phase separation studied by this technique, which is very important for us to understand and control the surface morphology and structure, has been discussed. The critical surface phase separation temperature for a 50/50 PMMA/SAN blend film is found to be around 165 °C. From the power law of $q^*(t) \sim t^{-n}$, two distinct regimes are found through the whole investigated time scale after the thin films abruptly jumped to an unstable state. The early stage probably is dominated by one component's diffusion to the surface, and the restriction of the surface geometry to chain mobility, resulting in much slower kinetics than those obtained from literature while the late stage obeyed the Lifschitz−Slyozov (LS) law.

Acknowledgment. This work is supported by the National Natural Science Foundation of China for the General (50373044, 50403008), Key (20334010), and Major (50390090, 20490220) Programs and the Chinese Academy of Sciences (KJCX2-SW-H07) and is subsidized by the Special Funds for Major State Basic Research Projects (No. 2003CB615600).

References and Notes

(1) Binder, K. *Adv. Polym. Sci.* **1999**, *138*, 1.
(2) Budkowski, A. *Adv. Polym. Sci.* **1999**, *148*, 1.
(3) Cahn, J. W.; Hilliard, J. E. *J. Chem. Phys.* **1958**, *28*, 258.
(4) Cook, H. E. *Acta Metall.* **1970**, *18*, 297.
(5) Lifshitz, I. M.; Slyozov, V. V. *J. Phys. Chem. Solids* **1961**, *19*, 35.
(6) Siggia, E. D. *Phys. Rev. A* **1979**, *20*, 595.
(7) Puri, S.; Binder, K. *Phys. Rev. Lett.* **2001**, *86*, 1797.
(8) Tanaka, H. *Phys. Rev. E* **1996**, *54*, 1709.
(9) Tanaka, H.; Araki, T. *Phys. Rev. Lett.* **1998**, *81*, 389.
(10) Tanaka, H. *J. Chem. Phys.* **1994**, *100*, 5323.
(11) Liu, H.; Bhattacharya, A.; Chakrabarti, A. *J. Chem. Phys.* **1999**, *111*, 11183.
(12) Thompson, P. A.; Grest, G. S.; Robbins, M. O. *Phys. Rev. Lett.* **1992**, *68*, 3448.
(13) Bhattacharya, A.; Mahanti, S. D.; Chakrabarti, A. *Phys. Rev. Lett.* **1998**, *80*, 333.
(14) Colombani, J.; Bert, J. *Phys. Rev. E* **2004**, *69*, 011402.
(15) Tokuyama, M.; Enomoto, Y. *Phys. Rev. Lett.* **1992**, *69*, 312.
(16) Fialkowski, M.; Aksimentive, A.; Holyst, R. *Phys. Rev. Lett.* **2001**, *86*, 240.
(17) Troian, S. M. *Phys. Rev. Lett.* **1993**, *71*, 1399.
(18) Laradji, M.; Toxvaerd, S.; Mouritsen, O. G. *Phys. Rev. Lett.* **1996**, *77*, 2253.
(19) Taniguchi, T.; Onuki, A. *Phys. Rev. Lett.* **1996**, *77*, 4910.
(20) Bates, F. S.; Wiltzius, P. *J. Chem. Phys.* **1989**, *91*, 3258.
(21) Kubota, K.; Kuwahara, N. *Phys. Rev. Lett.* **1992**, *68*, 197.
(22) Sung, L.; Karim, A.; Douglas, J. F.; Han, C. C. *Phys. Rev. Lett.* **1996**, *76*, 4368.
(23) Bruder, F.; Brenn, R. *Phys. Rev. Lett.* **1992**, *69*, 624.
(24) Shi, B. Q.; Harrison, C.; Cumming, A. *Phys. Rev. Lett.* **1993**, *70*, 206.
(25) Wiltzius, P.; Cumming, A. *Phys. Rev. Lett.* **1991**, *66*, 3000.
(26) Piazza, R.; Pierno, M.; Vignati, E.; Venturoli, G.; Francia, F.; Mallardi, A.; Palazzo, G. *Phys. Rev. Lett.* **2003**, *90*, 208101.
(27) Tanaka, H. *Phys. Rev. Lett.* **1994**, *72*, 3690.
(28) Tanaka, H. *Phys. Rev. Lett.* **1993**, *71*, 3158.
(29) Haas, C. K.; Torkelson, J. M. *Phys. Rev. Lett.* **1995**, *75*, 3134.
(30) Takeno, H.; Hashimoto, T. *J. Chem. Phys.* **1998**, *108*, 1225.
(31) Meyers, G. F.; DeKoven, B. M.; Seitz, J. T. *Langmuir* **1992**, *8*, 2330.
(32) Geoghegan, M.; Krausch, G. *Prog. Polym. Sci.* **2003**, *28*, 261.
(33) Wang, H.; Composto, R. J. *J. Chem. Phys.* **2000**, *113*, 10386.
(34) Zhang Newby, B.; Composto, R. J. *Phys. Rev. Lett.* **2001**, *87*, 098302.
(35) Muresan, A. S.; Diamant, H.; Lee, K. Y. C. *J. Am. Chem. Soc.* **2001**, *123*, 6951.
(36) Noy, A.; Zepeda, S.; Orme, C. A.; Yeh, Y.; Yoreo, J. J. D. *J. Am. Chem. Soc.* **2003**, *125*, 1356.
(37) Yang, G.; Woodhouse, K. A.; Yip, C. M. *J. Am. Chem. Soc.* **2002**, *124*, 10648.
(38) Magonov, S. N.; Yerina, N. A. *Langmuir* **2003**, *19*, 500.
(39) Gunning, A. P.; Mackie, A. R.; Wilde, P. J.; Morris, V. J. *Langmuir* **1999**, *15*, 4636.
(40) Schönherr, H.; Chechik, V.; Stirling, C. J. M.; Vancso, G. J. *J. Am. Chem. Soc.* **2000**, *122*, 3679.
(41) Doudevski, I.; Schwartz, D. K. *J. Am. Chem. Soc.* **2001**, *123*, 6867.
(42) Kaasgaard, T.; Leidy, C.; Ipsen, J. H.; Mouritsen, O. G.; Jørgensen, K. *Single Molecules* **2001**, *2*, 105.
(43) Hierlemann, A.; Campell, J. K.; Baker, L. A.; Crooks, R. M.; Ricco, A. J. *J. Am. Chem. Soc.* **1998**, *120*, 5323.
(44) Lackowski, W. M.; Campbell, J. K.; Edwards, G.; Chechik, V.; Crooks, R. M. *Langmuir* **1999**, *15*, 7632.
(45) Schönherr, H.; Waymouth, R. M.; Frank, C. W. *Macromolecules* **2003**, *36*, 2412.
(46) Hobbs, J. K.; Humphris, A. D. L.; Miles, M. J. *Macromolecules* **2001**, *34*, 5508.
(47) Beekmans, L. G. M.; Vallée, R.; Vancso, G. J. *Macromolecules* **2002**, *35*, 9383.
(48) Lei, Y. G.; Chan, C. M.; Li, J. X.; Ng, K. M.; Wang, Y.; Jiang, Y.; Li, L. *Macromolecules* **2002**, *35*, 6751.
(49) Basire, C.; Ivanov, D. A. *Phys. Rev. Lett.* **2000**, *85*, 5587.
(50) Zhou, W.; Cheng, S. Z. D.; Putthanarat, S.; Eby, R. K.; Reneker, D. H.; Lotz, B.; Magonov, S.; Hsieh, E. T.; Geerts, R. G.; Palackal, S. J.; Hawley, G. R.; Welch, M. B. *Macromolecules* **2000**, *33*, 6861.
(51) Wang, H.; Composto, R. J. *Interface Sci.* **2003**, *11*, 237 and references therein.
(52) Wen, G.; Li, X.; Liao, Y.; An, L. *Polymer* **2003**, *44*, 4035.
(53) Buschbaum, P. M.; O'Neil, S. A.; Affrossman, S.; Stamm, M. *Macromolecules* **1998**, *31*, 5003.
(54) Ma, Y. Q. *J. Chem. Phys.* **2001**, *114*, 3734.

MA0487305